# Ion Mobilities in Supercritical Ethane, Xenon, and Carbon Dioxide

**Kengo Itoh**

*Department of Pure and Applied Science, University of Tokyo, Tokyo 153-8902, Japan*

**Richard A. Holroyd***

*Chemistry Department, Brookhaven National Laboratory, Upton, New York 11973*

**Masaru Nishikawa**

*Faculty of Engineering, Kanagawa Institute of Technology, 1030 Shimo-Ogino, Astugi 243-0292, Japan*

*Received: September 23, 2000; In Final Form: November 28, 2000*

The mobility of positive ions was measured in supercritical ethane, xenon, and carbon dioxide as a function of pressure at several temperatures. In supercritical $CO_2$ the mobility of negative ions was also measured. Radii of the moving clusters were calculated with a hydrodynamic compressible continuum model that takes the enhancement in density and viscosity near the ions into account. The results show that positive ions move with a large solvation shell. Changes in size of this shell occur as a function of temperature and pressure. The largest radii at each temperature are found to occur at the pressure corresponding to the maximum in the isothermal compressibility. For positive ions the first solvation shell is totally filled under all conditions.

## Introduction

Measurements of ionic mobilities ($\mu$) in supercritical fluids are of interest not only to understand ion transport but also because this information can help in the interpretation of charge transfer and ionic reactions. For such reactions the rate constants often approach the diffusion rate.[1−3] The rate constant of diffusion-controlled reactions can be calculated from the diffusion coefficient of ions and the latter can be derived from the mobility using the Einstein relation $D = \mu k_B T/e$.

Mobilities also provide information on the size of the mobile ion clusters. It is already known that large volume changes occur due to electrostriction when an ion is introduced into a SC fluid. This has been demonstrated in our laboratory by pulse conductivity studies of ethane solutions.[4−6] Compressible continuum model calculations reported in those studies reveal the extent of density buildup near ions.

The size of the cluster that actually moves with the ion is deduced from the mobility in this study. A similar analysis was done for measurements of the mobility of $O_2^-$ in neon, at a temperature 0.6 K above $T_c$.[7] Our analysis takes into account the electrostriction that results not only in a buildup of density but also an increase in viscosity around the ion. The hydrodynamic problem of determining the radius of the cluster, $r_c$, must consider this radial distribution of density and viscosity around the ion. In the neon study Borghesani et al.used a Stokes-like formula:

$$r_c = e/6\pi\eta\mu f \qquad (1)$$

where $\eta$ is the bulk viscosity and $f$ a correction term. This term was between 1 and 2 and showed a maximum at a density close to the critical density. The best fit to the data indicated $r_c = 0.4$ nm, which suggests the ion moves with one nearly complete solvation shell. A similar study was made of $O_2^-$ in argon also at a temperature 0.6 K above $T_c$[8] by the same group. They found $r_c$ to increase with both density and isothermal compressibility, the latter term being important only close to the critical density. The viscosity used in eq 1 was evaluated at a fixed distance from the ion. The results indicate the $O_2^-$ ion moves with a large solvation shell. Another evaluation of the Ne results proposed by Volykhin et al.[9] takes into account the short-range repulsion of the weakly bound electron of the negative ion, which leads to the formation of a cavity around the anion in this fluid. The mobility could then be accounted for by using Stokes' equation where the radius and viscosity are taken at the point where the density reaches a maximum.

Our emphasis here is on positive ions and in determining the size of the mobile ion clusters in SC fluids using our compressible continuum model[4,5] to determine density and viscosity in regions surrounding the ion. Previous studies of ion mobilities in ethane,[10] $CO_2$,[11] and Xe[12] in the density region near critical densities were done either at lower temperatures ($T \leq T_c$) or at lower pressures ($P \leq P_c$). Here we report information about ion transport for $T > T_c$, where the pressure has been varied isothermally.

## Experimental Section

Ethane (MG Industries, scientific grade) was purified by passage through the appropriate Pall filter. $CO_2$ was from Alphagaz (99.998%) and was used as received. The level of oxygen impurity is reported to be <2 ppm. Xenon was scientific grade from MG Industries and was purified by passage through a Pall filter.

In the pulse conductivity technique used, the sample is exposed to a pulse of X-rays generated by impinging a 0.06−2.0 $\mu$s pulse of electrons from a 2 MeV Van de Graaff accelerator on a lead target. The sample cell for the SC fluid has been described elsewhere.[4] The signal from the cell was fed to a current amplifier (Kiethley model 428) using gains of $10^7$−$10^8$ V/A, and a time response of 30 $\mu$s. The output of the amplifier was fed to a transient recorder (Lecroy, 6103). A

10.1021/jp003451e CCC: $20.00

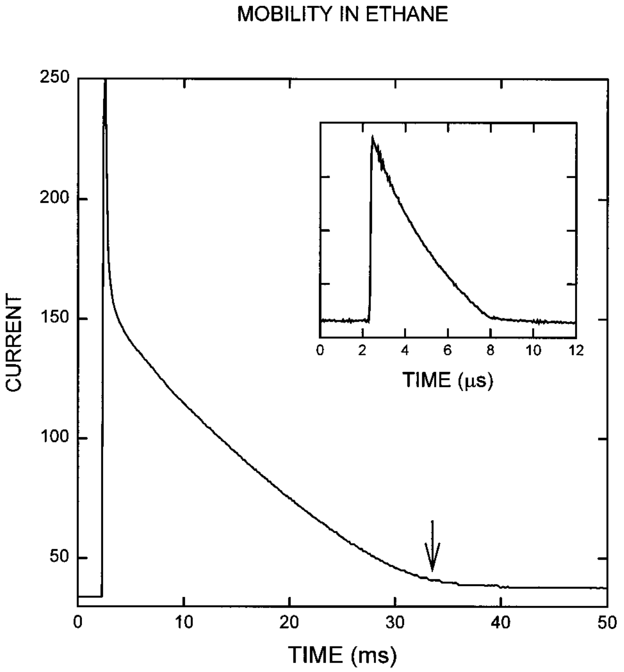

**Figure 1.** Conductivity trace for ethane at 33 °C and 93.2 bar for $E = 5350$ V/cm. Inset: trace for electron in the same sample using a fast amplifier for $E = 2510$ V/cm.

typical drift trace observed for ethane is shown in Figure 1. The "spike" at early times is attributed to the electron. It is not well resolved because of the long time constant. The inset shows the electron signal at short times for the same sample using a fast amplifier.

To obtain results for positive ions in the case of ethane and xenon, electron-attaching impurities had to be reduced to a sufficiently low level so that the electrons were drawn out by the field and negative ions not formed. For this reason measurements of both the electron lifetime ($\tau_e$) and electron mobility ($\mu_e$) or drift time ($\tau_d$) were made at each pressure and temperature by the method described earlier.[4] For ethane $\mu_e$ decreases from values $>50$ cm$^2$/(V s) in the critical region to values near 10 cm$^2$/(V s) at high pressure.[13] For Xe the electron mobility behaves oppositely, increasing with pressure; however, as shown in Figure 2, the dependence of the drift velocity ($v_D$) on the field ($E$) is nonlinear. At the highest density studied $v_D$ increases to a maximum of $7.2 \times 10^5$ cm/s at 1.5 kV/cm and then decreases at higher field. This maximum is more than twice the maximum for liquid Xe reported for a lower temperature and higher densities.[14] The dependence of $v_D$ on $E$ is independent of temperature at each density in SC Xe. As the density decreases, the peak value of $v_D$ becomes less and the curves become concave upward at low field. All curves tend to a plateau value for fields above 6 kV/cm.

It was required for all measurements that $\tau_e/\tau_d \gg 1$ where $\tau_e$ is the electron lifetime relative to capture by impurities and $\tau_d$ is the electron drift time, given by $d/v_D$. For the cell used the plate separation $d$ is 0.299 cm. Points where $\tau_e/\tau_d$ was close to 1 were discarded. In both Xe and ethane, $2 < \tau_e/\tau_d < 10$; thus the percentage of electrons that drifted to the anode was more than 85%.

For ethane the density was determined using an EOS by Younglove et al.[15] and the viscosity using an equation by Friend et al.[16] For CO$_2$ the density was determined using an EOS by Ely[17] and the viscosity from the correlation by Chung.[18] For xenon both the NIST Database 12[19] and an EOS by Sifner and Klomfer[20] were employed.

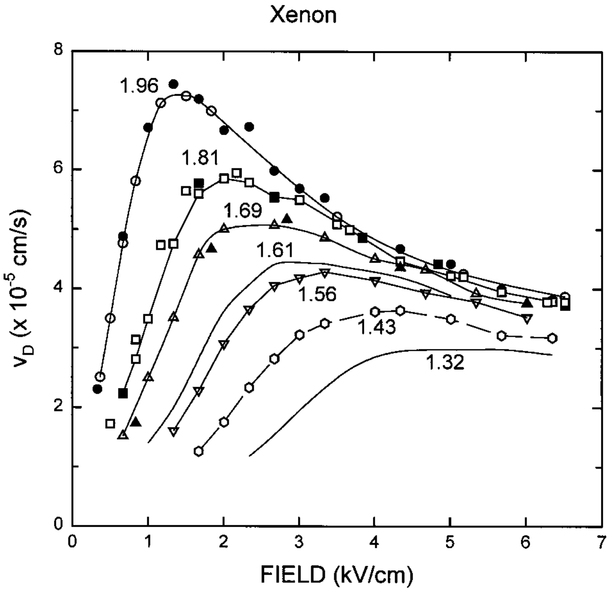

**Figure 2.** Drift velocity, $v_D$, versus electric field for SC Xe at indicated densities in g/cm$^3$. For the top three lines, the solid points are for 25 °C; other points for other temperatures. Data for lower four lines obtained at 18 °C.

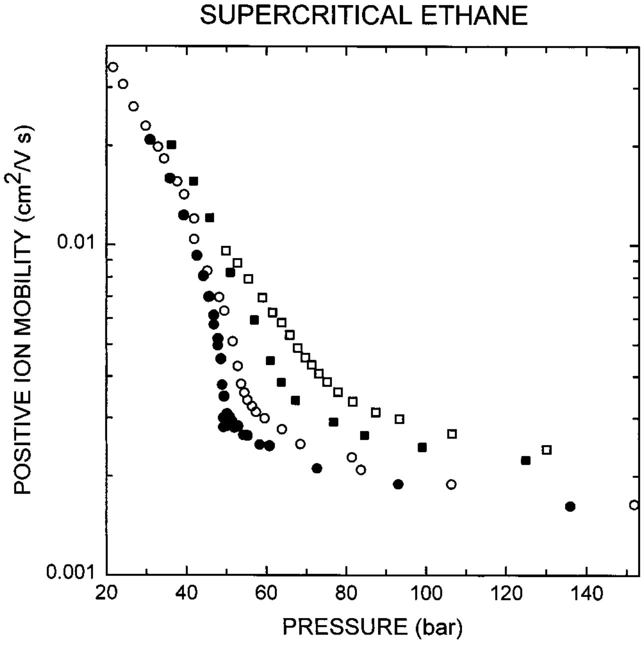

**Figure 3.** Mobility of positive ions in ethane versus reduced density: (●) 33 °C; (○) 37 °C; (■) 45 °C; (□) 53 °C.

## Results

**Ethane ($T_c$ = 32.3 °C).** Figure 3 shows the pressure dependence of the mobility of positive ions in SC ethane at four temperatures. The mobility generally decreases with increasing pressure. There is little temperature dependence at any one pressure except in the critical region. Diffusion coefficients of the positive ion were calculated using the Einstein relation, and the results are shown in Table 1.

**Xenon ($T_c$ = 16.6 °C).** Figure 4 shows the positive ion mobility in SC xenon at four temperatures. The mobility generally decreases with pressure, rather steeply at low pressures and more gradually at higher pressures. A minimum is actually observed at 18 °C and 60 bar. The mobility increases with temperature at all pressures. At 18 °C and high pressures the

**TABLE 1: Diffusion Coefficients[a] (*D*) for Positive Ions in SC Ethane**

| | temp, °C | | | |
|---|---|---|---|---|
| $\rho/\rho_c$ | 33 | 37 | 45 | 53 |
| 1.0 | | 1.06 | 1.16 | 1.28 |
| 1.2 | 0.808 | 0.931 | 0.984 | 1.05 |
| 1.4 | 0.738 | 0.798 | 0.829 | 0.87 |
| 1.6 | 0.642 | 0.659 | 0.697 | 0.735 |
| 1.8 | 0.531 | 0.513 | 0.586 | 0.646 |

[a] units of *D* are $10^{-4}$ cm²/s.

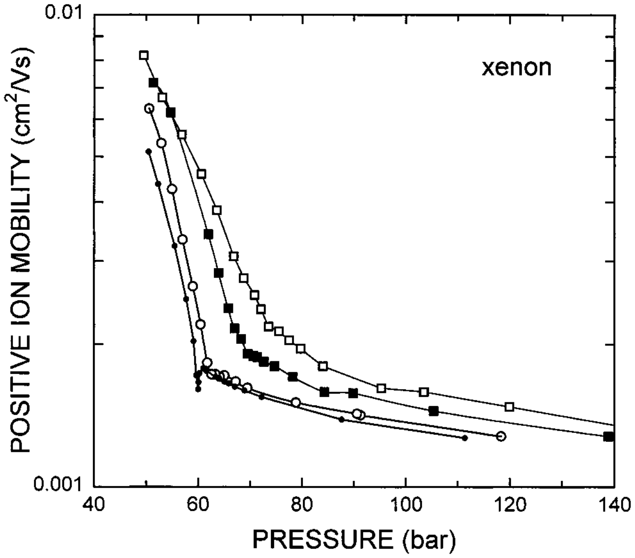

**Figure 4.** Mobility of positive ions in xenon: (●) 18 °C; (○) 20 °C; (■) 25 °C; (□) 30 °C.

**TABLE 2: Diffusion Coefficients[a] (*D*) for Positive Ions in SC Xenon**

| | temp, °C | | | |
|---|---|---|---|---|
| $\rho/\rho_c$ | 18 | 20 | 25 | 30 |
| 1.0 | | 0.436 | 0.505 | 0.561 |
| 1.2 | 0.427 | 0.437 | 0.479 | 0.511 |
| 1.4 | 0.423 | 0.415 | 0.438 | 0.454 |
| 1.6 | 0.339 | 0.368 | 0.382 | 0.388 |
| 1.8 | | | 0.312 | 0.315 |

[a] units of *D* are $10^{-4}$ cm²/s.

mobility of the positive ion is $1.3 \times 10^{-3}$ cm²/(V s). In liquid Xe the positive hole moves by hopping and the mobility is higher; e.g., $4.1 \times 10^{-3}$ at 7 °C.[21] However, this hole mobility decreases rapidly as the temperature increases and as the density decreases, which probably accounts for the lack of observation of this mechanism of transport in SC Xe. Diffusion coefficients are generally lower than for ethane as shown in Table 2.

**$CO_2$ ($T_c$ = 31.0 °C).** For $CO_2$ quite different conductivity traces were observed depending on the pressure. Above $P_c$ two breaks were observed as shown in Figure 5a. Thus, there are two types of ions present with different drift times, as indicated by the arrows. The dotted line represents the current attributed to the slower ion. The areas of the two triangles are such that each class of ion contributes approximately 50% to the current, as expected if one were the positive and one the negative ion. The mobilities of these ions in $CO_2$ are shown for 306 and 313 K versus pressure in Figure 6.

At low pressures only one break in the conductivity trace was observed, as shown in Figure 5b. Thus, the two classes of ions have the same mobility. This is consistent with the study[22] done near one bar, which reported equal mobilities for the positive and negative species. At densities below $0.2\rho_c$ the negative ion exhibits higher mobilities due to an electron attachment−detachment equilibrium with $CO_2$.[11,23] Our work did not extend down to such low densities. There was no evidence of such a fast species at the higher densities and pressures studied here.

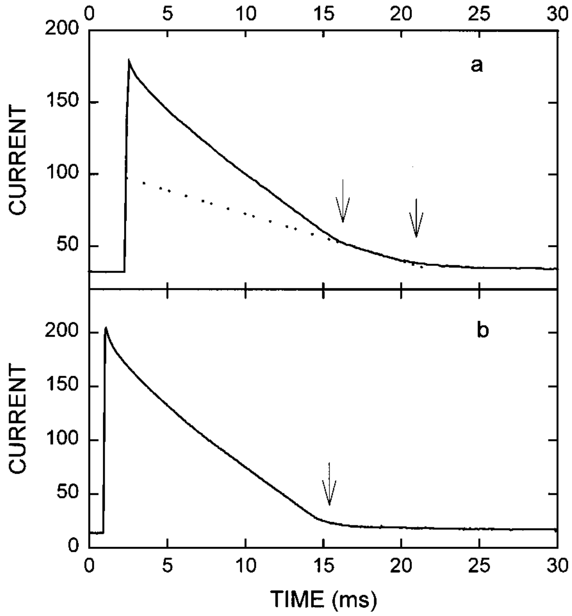

**Figure 5.** Conductivity traces for $CO_2$ at 33 °C: (a) 84 bar and $E$ = 6.35 kV/cm; (b) 69 bar and $E$ = 3.34 kV/cm.

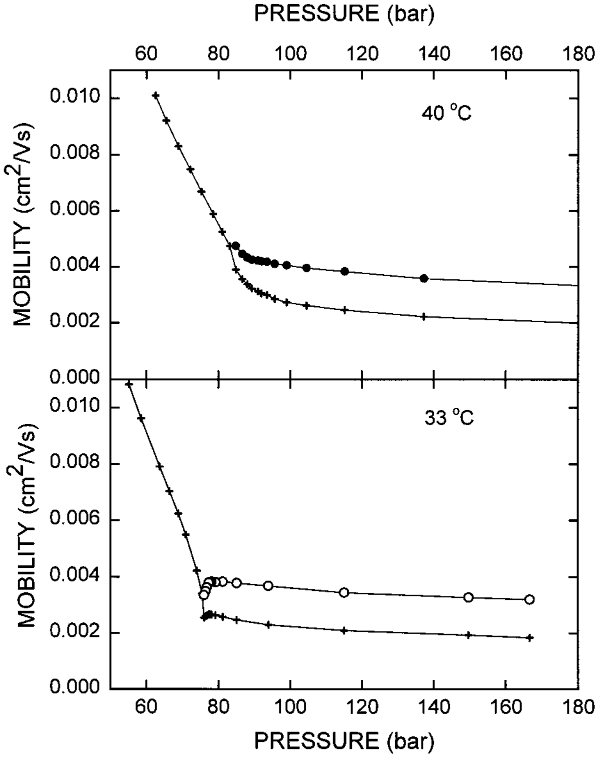

**Figure 6.** Mobility of ions in $CO_2$ versus density: top 40 °C; bottom 33 °C: (+) slow ion; (○, ●) fast ion.

Although the sample of $CO_2$ used was quite pure, it was not degassed or further purified prior to use. Since oxygen is likely to be present and since it is a product of the irradiation of $CO_2$[24] and also considering the duration of the drift experiment, it is likely that some electrons will end up on oxygen. Diffusion coefficients of the ions, calculated from the mobilities, are shown

**TABLE 3: Diffusion Coefficients ($D$)[a] for Ions in SC Co$_2$**

| | temp, °C | | | | |
|---|---|---|---|---|---|
| | 33 | | 40 | | 50[b] |
| $\rho/\rho_c$ | ion(1) | ion(2) | ion(1) | ion(2) | NQ$^-$ |
| 1.0 | 0.986 | 0.707 | 1.14 | 0.874 | |
| 1.2 | 1.02 | 0.700 | 1.12 | 0.795 | 0.92 |
| 1.4 | 1.00 | 0.661 | 1.07 | 0.709 | 0.82 |
| 1.6 | 0.945 | 0.590 | 0.985 | 0.615 | 0.66 |
| 1.8 | 0.844 | 0.488 | 0.868 | 0.514 | 0.51 |

[a] Units of $D$ are $10^{-4}$ cm$^2$/s. [b] Reference 25.

in Table 3. The results obtained for the naphthoquinone anion at 323.2 K[25] are closer to the values obtained here for the slower species, ion(2).

## Discussion

As indicated in the Introduction, the hydrodynamic analysis of the motion of ions in a SC fluid must take into account the radial dependence of the density and viscosity in order to calculate the size of the moving cluster. There is ample evidence of enhanced density around ions both from our own studies of electron attachment to solutes in SC ethane,[4-6] and from studies of ion mobility in SC neon[7] and argon.[8] Also the compressible continuum model calculations show the radial dependence of the density buildup, due to electrostriction. The viscosity should show a similar radial dependence, as was reported for neon,[7] being higher near the ion and decreasing to the bulk value a few nm from the ion.

**Hydrodynamic Compressible Continuum Model.** An extension of the compressible continuum model described earlier[4,5] is used here to derive the size of the moving cluster from the ion mobility. In our calculation the viscous drag on a hard sphere, of radius r$_c$ with a unit charge, is derived using the basic equation of motion for a compressible fluid:[26]

$$\partial \mathbf{J}/\partial t = 0 = -\nabla\left(\frac{\mathbf{JJ}}{\rho}\right) - \nabla P_{\text{total}} - \nabla\tau + \frac{1}{2}(\epsilon_r - 1)\epsilon_0 \nabla E_{\text{ion}}^{\ 2} \tag{2}$$

where $\mathbf{J}$ is the fluid flow and the shear stress tensor, $\tau$, is given by

$$\tau = -\eta(\nabla \mathbf{v}^t + (\nabla \mathbf{v}^t)^t) + \frac{2}{3}\eta \,\text{div}\, \mathbf{v}, \qquad \boldsymbol{J} = \mathbf{v}\rho \quad \text{and} \quad \mathbf{v}^t = (v_x, v_y, v_z) \tag{3}$$

and the equation of continuity,

$$\text{div}\, \mathbf{J} = 0 \tag{4}$$

The velocity of the flow is $\mathbf{v}$ and the radial changes in density ($\rho_r$), viscosity ($\eta_r$) and dielectric constant ($\epsilon_r$) around the ion are taken into account. For the purpose of calculation we consider the ion at rest with the fluid flowing around to simulate the motion of the ion in the direction of the applied electric field. The possibility exists that due to the motion some additional buildup in density will occur on the upstream of the ion and some lowering of the density downstream.

Practical calculations were made as follows. As a starting point the medium is assumed to be uniform. Then an approximate value of the hard sphere radius is chosen. From the density at each point, the dielectric constant, $\epsilon_r$, is calculated from the Clausius–Mosotti equation as a function of distance, $r$, from the ion and as a function of the angle, $\theta$, from the direction of the applied field. The field, $E_{\text{ion}}$, is calculated using this $\epsilon_r$ and the field contribution to the total pressure $P_{\text{total}}$ calculated by

$$\nabla P_{\text{charge}} = \frac{1}{2}(\epsilon_r - 1)\epsilon_0 \nabla E_{\text{ion}}^{\ 2} \tag{5}$$

Also the viscosity is calculated at each point and used to evaluate $\mathbf{J}$ using the continuity equation and the curl of the equation of motion: curl $[\nabla(\mathbf{JJ}/\rho) + \nabla\tau] = 0$. From $\mathbf{J}$, the contribution to the pressure from the fluid flow

$$\nabla P_{\text{flow}} = -\nabla\left(\frac{\mathbf{JJ}}{\rho}\right) - \nabla\tau \tag{6}$$

is calculated from eq 6. Then $\nabla P_{\text{total}} = \nabla P_{\text{flow}} + \nabla P_{\text{charge}}$ is integrated to obtain the new pressure. A new value of the density is calculated from this new pressure, and the process is iterated until there is no change in the parameters.

Then the force, $F$, exerted on the sphere from the flow is calculated from the pressure $P$ and the tangential component of the shear stress $\tau_{r\theta}$ using

$$F = -\pi r_c^{\ 2} \int_0^{2\pi} P(r{=}r_c) \cos\theta \sin\theta \, d\theta + \pi r_c^{\ 2} \int_0^{2\pi} \tau_{r\theta}(r{=}r_c) \sin^2\theta \, d\theta \tag{7}$$

where the first term is the form drag and the second term the friction drag. A trial mobility, $\mu$, is then calculated from

$$\mu = \frac{ev}{F} \tag{8}$$

A new value of $r_c$ is chosen, and the whole calculation is repeated until the experimentally observed mobility value is obtained. No approximations are made in the calculation. At low densities, difficulties were frequently encountered due to lack of convergence.

**Xenon.** Application of our hydrodynamic compressible continuum (HCC) model to the xenon data gives the results shown by the points in Figure 7a. The calculated radii of the moving clusters are near 0.6 nm at pressures above 75 bar for all temperatures from 18 to 30 °C. This radius corresponds to approximately one completely filled solvation shell, since the diameter of xenon is 0.405 nm.[18] Closer inspection reveals that at high pressure the cluster size decreases slightly with increasing temperature, from 0.615 nm at 18 °C to 0.58 nm at 30 °C. At lower pressures the clusters grow much larger, as shown. The maxima in cluster sizes occur at pressures where the compressibility, shown in Figure 7b, maximizes at each temperature. As the temperature increases, the heights of the maxima decrease; that is, the clusters become smaller. These xenon atoms clustered around the ion are considered to be static since they move with the ion.

There is a correspondence of cluster size with the magnitude of the compressibility. This is not surprising considering the volume changes observed in electron attachment reactions in SC ethane.[5,6] These volume changes are related to electrostriction around the negative ion, and the changes are the largest in regions of high compressibility.

Previous studies have evaluated the viscosity at a given fixed distance from the ion. In the study of the mobility of O$_2^-$ in fluid Ar the distance used was 1.85 nm.[8] In the study of the mobility of O$_2^-$ in fluid Ne, where a hollow cavity is expected around the ion, the viscosity was chosen at the distance corresponding to the density maximum, or 0.53 nm.[9] In our

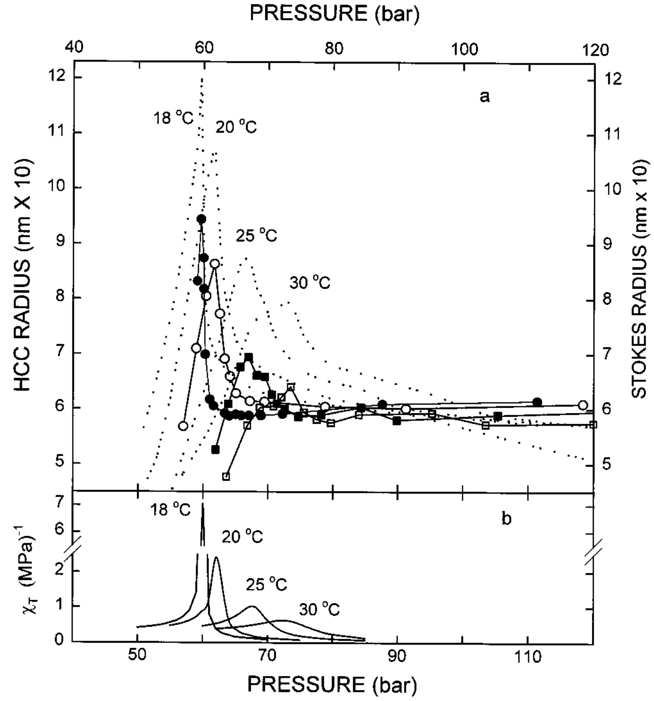

**Figure 7.** (a) Positive ion radii ($r_c$) of clusters in Xenon evaluated with the HCC model: (●) 18 °C; (○) 20 °C; (■) 25 °C; (□) 30 °C. Dotted lines are radii ($r_s$) from Stokes' eq. (b) Compressibility of Xe at indicated temperatures.

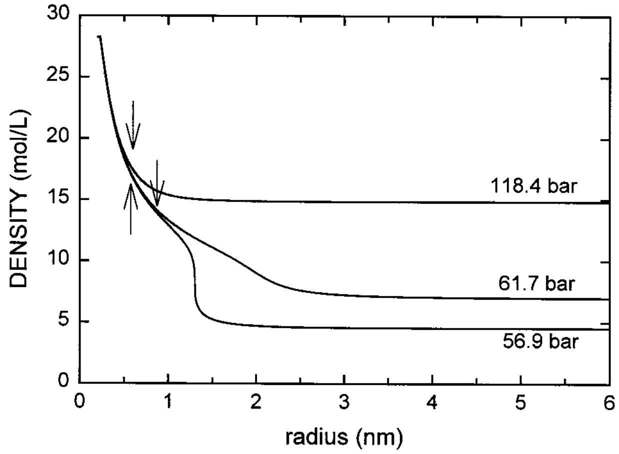

**Figure 8.** Density profiles around $Xe^+$ in SC Xe at 20 °C and the pressures indicated. Arrows indicate HCC radii at corresponding pressure.

HCC model the variation in viscosity as a function of distance from the moving ion is taken into account.

Radii were also calculated using Stokes' eq 9 and values of the bulk viscosity. These results are shown by the dotted lines in Figure 7a.

$$r_s = e/6\pi\eta\mu \qquad (9)$$

Qualitatively, the pressure dependence is the same, $r_s$ is comparable to $r_c$ at high pressure, but the cluster sizes are larger in the high compressibility regions.

The density profile around a $Xe^+$ ion in SC Xe, as calculated using the compressible continuum (CC) model,[4] depends on pressure. Results for three different pressures are shown in Figure 8 for 20 °C. Calculations using the HCC model gave the same profile, independent of $\theta$. This is because the drift velocity values used in the HCC calculation are very small (≈0.1 m/s), which matches the experimental conditions. The arrows in Figure 8 indicate the radius of the moving clusters ($r_c$) calculated with the HCC model. At high pressure the density drops to bulk density just outside of $r_c$. In this case most of the region of enhanced density moves with the ion. At lower densities this is not the case. For 61.7 bar, which corresponds to the peak radius at this temperature, $r_c$ is 0.863 nm but there is considerable density buildup around the ion as far out as 2 nm. Similarly at 56.9 bar, the lowest pressure for which calculations were made at 20 °C, $r_c$ is 0.668 nm and there is enhancement in density as far out as 1.3 nm. This region, which encompasses the second and third solvation shells although more dense than the bulk region, does not move with the ions according to the model, and this outer region of the density buildup can be considered dynamic.

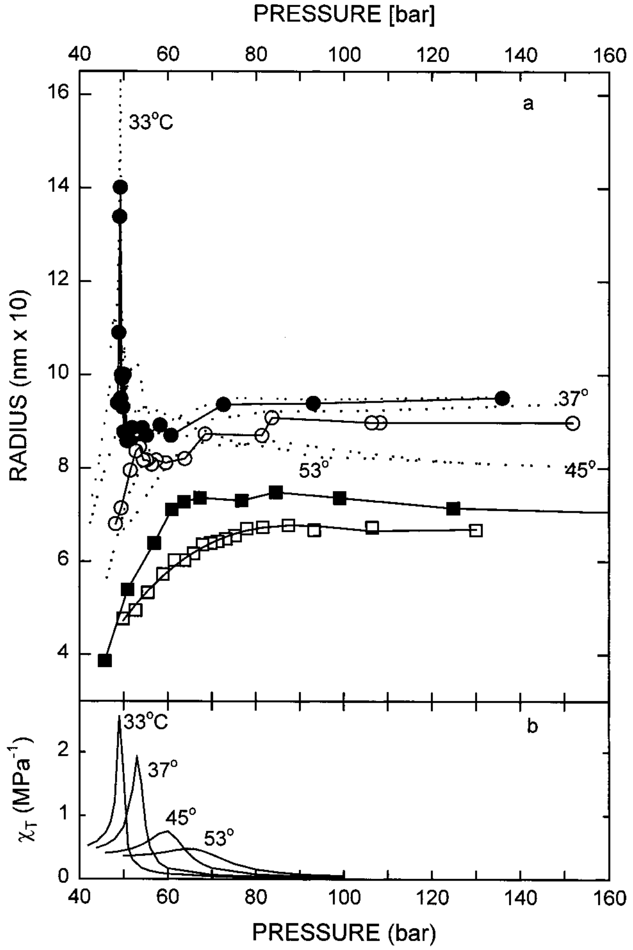

**Figure 9.** (a) Positive ion radii ($r_c$) of clusters in ethane evaluated with HCC model, which considers enhanced local density as well as viscosity: (●) 33 °C; (○) 37 °C; (■) 45 °C; (□) 53 °C. Dotted lines are radii ($r_s$) from the Stokes' equation. (b) Compressibility of ethane at indicated temperatures.

As mentioned above, not only the density but also the viscosity increases around an ion. The HCC model calculations for Xe indicate that the viscosity increases, as the distance from the ion decreases, in a manner quite similar to the density, as shown in Figure 8. Regions of enhanced viscosity extend at some pressures to ∼2 nm.

**Ethane.** The points in Figure 9a show the results of applying the HCC calculation to the ethane mobility data. The cluster radii are nearly constant at high densities but decrease in size with increasing temperature. The radius of 0.7 nm, observed at the higher temperatures and high pressure, corresponds to one

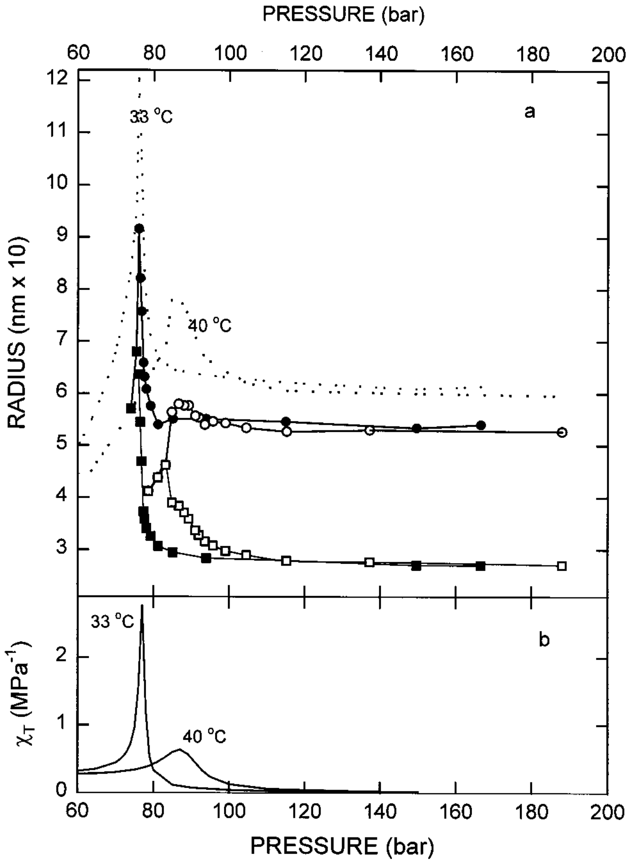

**Figure 10.** (a) Radii ($r_c$) of clusters around the ions in $CO_2$ evaluated with the HCC model versus pressure: slow ion (●) 33 °C, (○) 40 °C; fast ion (■) 33 °C, (□) 40 °C. Dotted lines are Stokes' radii for slow ion at indicated temperatures. (b) Compressibility of $CO_2$ at indicated temperatures in °C.

completely packed shell of ethane molecules around the ion, since the diameter of an ethane molecule is approximately 0.42 nm.[27] At lower temperatures the radii are larger, indicating partial filling of another solvation shell around the ion. Larger clusters are found in the region of high compressibility at 33 °C (compare Figure 9a,b).

Radii were also calculated from the ion mobility data for ethane using Stokes' equation (9) and the bulk value of the viscosity. At the two higher temperatures the cluster sizes do not change much in the SC region. The radii are close to 0.8 nm at high pressure. At 33 and 37 °C the radii are slightly higher, about 0.9 nm, at high pressures, but increase to larger values in the region near $P_c$ (see dotted lines in Figure 9a).

Density profiles around the positive ion in ethane are not expected to differ much from those calculated with the compressible continuum model for negative ions.[4] As in the case of sc Xe the density outside $r_c$ at high pressure is close to the bulk value. For example at 93 bar and 33 °C, $r_c$ is 0.94 nm and the density at this distance is only 5% above the bulk value. As observed for Xe, this is not the case at lower pressure. At 49.2 bar where $r_c$ is 1.4 nm, the density at this point is 72% above the bulk value of 5.68 mol/L. Thus, it appears that only the region of dense solvent close to the ion moves with it.

**$CO_2$.** The points in Figure 10a show the results of applying the HCC model to the ions in $CO_2$. There are some similarities to the xenon results in that at high densities the clusters do not change size with temperature and that the moving clusters become larger at intermediate densities; again the maxima occur at the compressibility maxima (see Figure 10b). The clusters are smaller than those in either ethane or xenon. The radius is 0.54 nm for the slower ion at high densities. The clusters would be expected to have radii of about 0.59 nm if the first solvation shell were filled considering the size of $CO_2$.[18] The radii of clusters calculated from the slower ion mobility data using bulk viscosities and eq 9 are shown by the dotted lines. This comparison shows clearly that the use of bulk viscosity exaggerates cluster size at all densities but particularly in the intermediate density region.

The mobility values for the faster ion suggests a smaller hydrodynamic radius at high densities. However, the HCC model calculations show that the cluster around this ion also grows at intermediate densities where the compressibility is high, an effect attributed to electrostriction, and then has the same size as the other ion at and below the density corresponding to the compressibility maximum.

The negative ion species in irradiated $CO_2$ gas has been suggested[22] to be $CO_4^-$ and the initial positive ion species has been identified in pulse radiolysis of supercritical $CO_2$ as $C_2O_4^+$.[2] We have not identified the ions; however, since $O_2$ may be present as an impurity and is formed by the radiation, electrons would be expected to transfer to $O_2$ during the drift time of 10−20 ms. Electron transfer from anions to solutes in supercritical $CO_2$ has been reported to be diffusion-controlled, and charge transfer from $C_2O_4^+$ to oxygen occurs rapidly in $CO_2$.[28] On the basis of this information, transfer to trace $O_2$ would be complete within a few microseconds forming $O_2^-$ (or $CO_4^-$) and $O_2^+$ (or $CO_4^+$). On the basis that negative ions, including $O_2^-$, generally have higher mobilities in liquids,[29−31] we suggest that the faster ion is the anion.

Both positive and negative ions will have clustered solvent molecules around them. According to the CC model, electrostriction is independent of the sign of the charge and not very sensitive to the radius of the ion. However, Volykhin et al.[9] have suggested that the short range (Pauli) repulsive interaction of the extra electron on the anion with the electrons in the neutral molecules of the fluid must also be taken into account. In this way the high mobility of $O_2^-$ in liquid Ne and He could be accounted for. This idea has been applied recently to other liquids.[30b,32] The positive ion lacks this repulsive potential and the solvent packs tightly in a solvation shell around the ion. The anion moves with less of the solvation shell, because of this repulsive term. This effect may apply equally well to supercritical fluids. The fast ion in $CO_2$, may be an example. The results show that at high pressures the hydrodynamic radius of the ion is small, $r_c = 0.28$ nm.

## Conclusion

The results on ion mobilities have been interpreted in terms of a Stokes-like model (HCC), which takes the high viscosity and density in the vicinity of the ion into account and derives the size of the moving clusters. These clusters are nearly constant in size throughout much of the SC region but grow dramatically in the near critical region where there is a correlation of cluster size with compressibility. In $CO_2$ there are two types of ions; the mobility of the faster ion, which may be $O_2^-$, is attributed to the small size of the moving cluster. Further work will be required to verify this identification. It will be interesting to see if other anions have higher mobilities than do cations in this and other SC fluids.[33]

**Acknowledgment.** This research was carried out at Brookhaven National Laboratory and supported under contract DE-AC02-98-CH10886 with U.S. Department of Energy and supported by its Division of Chemical Sciences, Office of Basic Energy

Sciences. K.I. and M.N. are supported by a Grant in Aid for Scientific Research from the Ministry of Education, Science, and Culture, Japan.

## References and Notes

(1) Takahashi, K.; Jonah, C. D.*Chem. Phys Lett*. **1997**, *264*, 297.

(2) Dimitrijevic, N. M.; Bartels, D. M.; Jonah, C. D.; Takahashi, K. *Chem. Phys. Lett*. **1999**, *309*, 61.

(3) Zhang, J.; Connery, K. A.; Brennecke, J. F.; Chateauneuf, J. E. *J. Phys. Chem.* **1996**, *100*, 12394.

(4) Holroyd, R. A.; Nishikawa, M. Itoh, K. *J. Phys. Chem. A* **1999**, *103*, 550.

(5) Nishikawa, M.; Itoh, K.; Holroyd, R. A. *J. Phys. Chem. B* **1999**, *103*, 9205.

(6) Holroyd, R. A.; Nishikawa, M.; Itoh, K. *J. Phys. Chem. B* **2000**, *104*, 11585.

(7) Borghesani, A. F.; Neri, D.; Santini, M. *Phys. Rev. E* **1993**, *48*, 1379.

(8) Borghesani, A. F.; Neri, D.; Barbarotto, A. *Chem. Phys. Lett*. **1997**, *267* 116.

(9) Volykhin, K. F.; Khrapak, A. G.; Schmidt, V. F. *JETP* **1995**, *81*, 901.

(10) Gee, N.; Freeman, G. R. *Can. J. Chem*. **1980**, *58*, 1490.

(11) Jacobson, F. M.; Freeman, G. R. *J. Chem. Phys*. **1986**, *84*, 3396.

(12) Gee, N.; Huang, S. S-S.; Wada, T.; Freeman, G. R. *J. Chem. Phys*. **1982**, *77*, 1411.

(13) Nishikawa, M.; Itoh, K.; Holroyd, R. A. Proceedings 13th International Conference on Dielectric Liquids, July, 1999, Nara Japan.

(14) Huang, S. S.-S.; Freeman, G. R. *J. Chem. Phys*. **1978**, *68*, 1355.

(15) Younglove, B. A.; Ely, J. F. *J. Phys. Chem. Ref. Data* **1987**, *16*, 577.

(16) Friend, D. G.; Ingham, H.; Ely, J. F. *J. Phys. Chem. Ref. Data* **1991**, *20*, 275.

(17) Ely, J. F. Supercritical Fluid Properties, Final Report. NTIS report D985011203; 1984.

(18) Reid, Robert, C.; Prausnitz, J. M.; Poling, Bruce, E. *The properties of gases and liquids*, 4th ed.; McGraw-Hill: New York, c1987.

(19) Friend, D. G. NIST Thermophysical Properties of Pure Fluids, Version 3.0, Database 12, 1992.

(20) Sifner, O.; Klomfer, J. *J. Phys. Chem. Ref. Data* **1994**, *23*, 63.

(21) Hilt, O.; Schmidt, W. F. *J. Phys. Condens Matter* **1994**, *6*, L735.

(22) Jówko, A.; Armstrong, D. A. *Radiat. Phys. Chem*. **1982**, *19*, 449.

(23) Warman, J. M.; Sowada, U.; Armstrong, D. A. *Chem. Phys. Lett*. **1981**, *82*, 458.

(24) Yosimura, M.; Chosa, M.; Soma, Y.; Nishikawa, M. *J. Chem. Phys*. **1972**, *57*, 1626.

(25) Kimura, Y.; Kanda, D.; Terazima, M.; Hirota, N. *J. Phys. Chem. B* **1997**, *101*, 4442.

(26) Bird, R. B.; Stewart, W. E.; Lightfoot, E. N. *Transport Phenomena*; John Wiley and Sons: New York, 1960.

(27) Ben-Amotz, D.; Willis, K. G. *J. Phys. Chem*. **1993**, *97*, 7736.

(28) Dimitrijevic, N. M.; Takahashi, K.; Bartels, D. M.; Jonah, C. D.; Trifunac, A. D. *J. Phys. Chem. A* **2000**, *104*, 568.

(29) Allen, A. O.; de Haas, M. P.; Hummel, A. *J. Chem. Phys*. **1976**, *64* 2587.

(30) Schmidt, W. F. *Liquid State Electronics of Insulating Liquids*; CRC Press: Boca Raton, FL, 1997; (a) p 119, (b) p 278.

(31) Schmidt, W. F.; Holroyd, R. A. *Radiat. Phys. Chem*. **1992**, *39*, 349.

(32) Khrapak, A. G.; Tegeder, P.; Illenberger, E.; Schmidt, W. F. *Chem. Phys. Lett*. **1999**, *310*, 557.

(33) Preliminary work indicates that the $C_6F_6^-$ anion has a higher mobility than the positive ion in supercritical Xe.